doi.org/10.36721/PJPS.2026.39.11.322.1

circ-ITCH suppresses prostate cancer cell proliferation, migration and invasion *in-vitro* through the miR-106b-5p/SETD2 axis

Junbin Jiang[1#], Jianwen Wei[1#], Feicheng Chen[2], Yutong Li[1], Longhong Ba[1*] and Bin Pan[1*]

[1]Department of Urology. The First Affiliated Hospital of Jinan University, Guangzhou, Guangdong 510632, China
[2]Department of Urology, Xinfeng People's Hospital, Shaoguan 511100, China

Abstract: **Background**: Prostate cancer (PCa) is one of the leading causes of male morbidity and mortality due to malignant disease throughout the world. Recently, circRNAs have been considered as important regulators in tumorigenesis related networks. Nevertheless, the biological role and expression pattern of circRNA-ITCH (circ-ITCH) in prostate cancer are still not fully understood. **Objectives**: The purpose of the present study was to determine circ-ITCH expression in prostate cancer tissues and cell lines and analyze its potential regulatory effects on the proliferation, apoptosis, migration and invasion of prostate cells *in-vitro*. **Methods**: The expression of circ-ITCH was detected in 6 pairs of PC tissues and adjacent normal tissues (n = 6) as well as PC cell lines by quantitative real-time PCR. The function of circ-ITCH was assessed by gain-of-function experiments. Cell proliferation and colony-forming efficiency were assessed using Cell Counting Kit-8 and plate cloning assays, respectively. The migratory and invasive abilities were examined via Wound Healing and Transwell assay and Annexin V-FITC/propidium iodide (PI) staining was used to assess apoptosis. Bioinformatic analysis in combination with dual-luciferase reporter analysis was performed to validate the regulatory relationships between circ-ITCH, miR-106b-5p and SETD2. **Results**: Relative to the corresponding control group, circ-ITCH expression was markedly decreased in prostate cancer tissues and cell lines. *In-vitro*, circ-ITCH overexpression inhibited cell proliferation and clonogenicity and increased the number of apoptotic cells in prostate cancer. Moreover, circ-ITCH overexpression reduced cell migration and invasion abilities. The luciferase reporter assays confirmed that circ-ITCH was the target of miR-106b-5p and miR-106b-5p targeted SETD2. circ-ITCH upregulation was correlated with elevated SETD2 expression, which is in line with a miR-106b-5p–dependent pattern of regulation. **Conclusion**: These findings suggest that circ-ITCH can modulate malignant cell phenotypes (proliferation, apoptosis, migration and invasion) in PCa cells *in-vitro* through the miR-106b-5p/SETD2 axis. There are only a limited number of tissue samples and *in-vitro* experimental designs in our study and more experiments will be needed to further confirm these findings and reveal the biological significance.

Keywords: Circ-ITCH; miR-106b-5p; Prostate cancer; SETD2

Submitted on 01-02-2026 – Revised on 21-02-2026 – Accepted on 22-02-2026

INTRODUCTION

Prostate cancer (PCa) is the second most commonly diagnosed cancer and still ranks as a major cause of male cancer-related deaths globally in men (Plym *et al.,* 2024; Sung *et al.,* 2021). Most prostate cancers grow slowly at initial stages, but a subset turns aggressive and advances to castration-resistant disease, for which there are currently no effective therapeutic options available. While early-stage PCa is typically asymptomatic and advanced-stage cancer can be a significant clinical burden associated with a (Zhu *et al.,* 2018; Lucarini *et al.,* 2023). This clinical variability emphasizes the importance of gaining a deeper understanding of the molecular mechanisms leading to progression and malignancy in prostate cancer.

Circular RNAs (circRNAs) are a family of endogenous noncoding RNA molecules with a circular covalently closed loop structure, which is devoid of both 5' cap and 3' poly (A) tail. This closed-loop confirms stronger stability of biological processes than line RNAs; circRNA plays a role in various processes, including oncogenesis and progression (Lindenberg *et al.,* 2017). A large proportion of circRNAs contain MREs and are thus miRNA regulate gene expression (13-15). In this way, circRNAs are not sponges to downstream target gene but indirectly translated into protein to modulate its expression (Fontana *et al.,* 2020; de Bono *et al.,* 2017).

It has been reported that circRNA–miRNA interactions modulate biological characteristics such as cell proliferation, apoptosis, migration, invasion and cancer in relevant studies (Hu and Guo, 2020). Yet, epigenetic regulation within this context depends on the biological functions of distinct circRNAs, which vary across different tumor types (Xu *et al.,* 2020). Although circCDR1as (also termed ciRS-7) has been well characterized in neurodevelopment and other cancers, its biological context is remarkably different from that of prostate cancer; thus, it is not applicable to deciphering PCa-specific circRNA regulation. On the other hand, RPs-linked circRNAs directly linked to TGFβ1/p-Smad2/3, such as circRNA-51217, which can promote prostate cancer cell invasion through signaling pathways (Yang *et al.,* 2018), deserve more attention.

**Corresponding author:* e-mail: panbin@jnu.edu.cn
#These authors contributed equally and are the co-first authors.

E3 circular RNA ITCH (Circ-ITCH) is derived from exons 7–14 of the itchy ubiquitin protein ligase (ITCH) gene through back-splicing. It is various other tumors, reported that circ-ITCH is also aberrantly expressed in diverse malignancies such as breast cancer, ovarian cancer, bladder cancer and prostate tumors, as well as plays an antioncogenic role (Hu *et al.,* 2018). Circ-ITCH acts as a "sponge" of the pathway inmicroRNA and suppresses Dvl2 to inhibit the Wnt/β-catenin signaling in esophageal squamous cell carcinoma (Wang *et al.,* 2019). These that circ-ITCH may act as a tumor suppressor through the regulation trends imply of post-transcription, but its targeting network and direct targets in prostate cancer are not completely understood.

Previous clinicopathological evidence showed that reduced circ-ITCH expression was correlated with worse clinicopathological characteristics and survival outcomes in prostate cancer patients who had radical prostatectomy (Huang *et al.,* 2019). However, the upstream regulatory mechanisms and downstream molecular targets of circ-ITCH in PCa have not yet fully elucidated. As noted previously, the definitive regulatory pathways involving circ-ITCH, miRNAs and mRNAs in the development of prostate cancer remain unclear.

There is mounting evidence that circRNAs directly participate in the biology of prostate cancer by influencing post-transcriptional networks, particularly through microRNA sequestering (Pan *et al.,* 2025). This circRNA–miRNA crosstalk can modulate core malignant cellular phenotypes, including cell viability-related metabolism, apoptosis, migration and invasion by relieving microRNA-mediated repression of their downstream targets (Siegel *et al.,* 2024). Crucially, the functional relevance of a specific circRNA is profoundly context-specific and regulatory axes discovered in other cancers should not be transferred to PCa without further investigation (Zhang *et al.,* 2024). Thus, the identification of PCa-relevant circRNA-implicated networks remains necessary for a more complete understanding of molecular processes that may promote aggressive phenotypes in cultured prostate cancer models (Zhou *et al.,* 2024).

In this study, the circ-ITCH/miR-106b-5p/SET domain-containing 2 (SETD2) axis has been investigated, as both SETD2 and miR-106b-5p have been reported to participate in tumor-related regulatory networks governing cell survival and migration (Kapper *et al.,* 2024). Then the bioinformatic resources (StarBase and UCSC Genome Browser used to predict complementary binding sites between miR-106b-5p Browser) were used, as well as SETD2, circ-ITCH and miR-106b-5p coupling endogenously, thereby indicating a potential relationship of regulation (Hu *et al.,* 2024). This study therefore (i) studied circ-ITCH expression in a small exploratory number of paired PCa tissues and in cell lines and (ii) investigated whether overexpression of circ-ITCH could be related to alterations of malignant cellular phenotypes (iii) assessing predicted RNA–RNA interactions *in-vitro*; while also experimentally with wild-type and mutant dual-luciferase reporter constructs (Nabar *et al.,* 2024). Overall, these experiments were not intended to prove an already established molecular mechanism but rather to provide evidence axis (Vidallon for a regulatory relationship in a candidate *et al.,* 2024).

The present study was designed to explore the expression of circ-ITCH in PCa tissues and cell lines and its possible regulatory effects on the proliferation, apoptosis, migration and invasion of PCa cells *in-vitro*. Herein, we aimed to further confirm the circ-ITCH/miR-106b-5p/SETD2 axis and explained its potential post-transcriptional regulatory networks. Nevertheless, our *in-vitro* findings still require more investigation and future clinical data will be needed to verify these conclusions.

MATERIALS AND METHODS

Tissue samples

Six paired PCa tissues and adjacent non-tumorous tissues (n = 6) were collected from patients who underwent radical prostatectomy in First Affiliated Hospital of Jinan University from 2020 to early 2021. This small sample size was adopted solely for preliminary exploratory analyses. All patients (age range, 56–86 years) received no chemotherapy, hormonal therapy or radiation therapy before surgery and their lesions were confirmed via pathological examination. Tissue samples were flash-frozen in liquid nitrogen and then stored at −80 °C for RNA isolation. All the participants provided written informed consent and this Committee (approval no. VPN/KY/20-95).

Cell culture and transfection

The Chinese Academy of Sciences Cell Bank gave us human prostatic epithelial cells (RWPE-1) and prostatic cancer cell lines (C4-2, VCaP, DU145, LNCaP, PC3 and BM-1604). all the cells grown in RPMI-1640 media (Life Technologies, Grand Island, NY) with 10% fetal bovine serum and 1% penicillin–streptomycin at 37 °C in a humidified incubator with 5% CO_2. Cell lines were routinely tested for mycoplasma and used for a limited number of passages to ensure experimental consistency. Plasmids overexpressing circ-ITCH and SETD2 were constructed using the pcDNA3.1 vector system. miR-106b-5p mimics and relative NC were purchased from a commercial supplier. Transfections were performed with Lipofectamine 3000 (Invitrogen) according to the manufacturer's instructions, using 2 μg of plasmid DNA and 50 nM of miRNA mimics per well.

Cell proliferation and assays of colony formation

For Cell Counting Kit-8 (CCK-8), 1 × 104 cells of C4-2 and DU145 cells were plated on the 96-well plate. At 24, 48, 72 and 96 h post-infection or virus sample treatment, CCK-8 reagent (10 μL) was added to each well and incubated for another 2 h. Abs at 450 nm were measured using a Microplate Reader (Molecular Devices, USA).

Background was subtracted using wells with medium only (blank) and the blank-subtracted absorbance was normalized to that of control cells. Metabolic activity, rather than total cell number, was quantified by relative absorbance. To assess colony formation, cells were seeded at 3×10^3 per well in 6-well plates and incubated for 11–14 days. The colonies were fixed in 4% paraformaldehyde, stained with 0.5% crystal violet and manually counted those that contained more than 50 cells (Hu and Guo, 2020).

Flow cytometry analysis of apoptosis

Apoptosis was analyzed by Annexin V–fluorescein isothiocyanate (FITC)/PI (propidium iodide) apoptosis detection kit (Beyotime), manufacturer's protocol. Cells were washed twice with phosphate-buffered saline (PBS) and resuspended in Annexin-binding buffer (without RNase A) containing standard concentrations of Annexin V-FITC and propidium iodide (PI) in the μg/mL range. After incubation for 15 min at room temperature in the dark, flow cytometric analysis was performed on a BD Biosciences instrument (BD Biosciences, Franklin Lakes, NJ, USA). Data were acquired from 10,000 events per sample and early- and late-apoptotic cell populations were identified using FlowJo software (v10.8, BD Biosciences).

Migration and invasion assays

For invasion, cells were transferred to Matrigel-coated (BD Biosciences, NJ) Transwell inserts (8-um pore size). A total of 5×10^4 cells in serum-free RPMI-1640 were seeded into the upper chamber, while the lower chamber contained RPMI-1640 supplemented with 10% fetal bovine serum (FBS) as a chemoattractant. After incubation for 48h, the cells that had invaded to the lower surface were fixed, stained with crystal violet and counted in five random fields per insert at 200x magnification. For migration assays, the same procedure was performed using uncoated Transwell inserts. For scratch wound-healing assays, cells were grown to confluence in culture dishes, a scratch was created using a sterile pipette tip and the cells were then incubated in serum-free medium to minimize proliferation effects. Photographs were taken at 0 and 24 h and the percentage reduction in the gap area due to wound healing was measured using ImageJ (version 1.54p) software to assess wound closure.

Luciferase reporter assay

Binding sequences between circ-ITCH or SETD2 and miR-106b-5p were first predicted by StarBase and then identified in the UCSC Genome Browser (http://genome.ucsc.edu/). The wild-type and mutant fragments of circ-ITCH and SETD2 3′-UTR with the mutations abrogating the binding of miR-106b-5p were synthesized and inserted downstream of the Renilla luciferase for psiCHECK-2 vector (Promega) carrying firefly luciferase as an internal control. For co-transfection experiments, C4-2 and DU145 cells were transfected with a reporter plasmid and miR-106b-5p mimics or negative controls. The activity of Renilla luciferase was normalized for firefly luciferase and the relative luciferase activity was determined with a dual-luciferase reporter assay system 24 h post-transfection. All the experiments were conducted in triplicate.

Quantitative real-time PCR (qRT-PCR)

Total RNA in the cells was extracted using TRIzol reagent and RNA purity was assessed by the A260/A280 ratio. The first strand of cDNA (complementary DNA) was synthesized with an M-MLV Reverse Transcriptase Kit. qRT-PCR was carried out on Bio-Rad CFX96 in GoTaq® qPCR Master Mix. B-Actin and U6 served as internal controls for SETD2 mRNA and miR-106b-5p, respectively, while circ-ITCH was the target of interest. Relative expression levels were calculated using the $2^{-\Delta\Delta Ct}$ method. All experiments were performed in replicates. A methodological limitation is that the divergent primers for circ-ITCH and the RNase R resistance assay have not yet been validated.

Western blot analysis

The RIPA lysis buffer was used to get the total protein, then separated it by 10% SDS-PAGE and put it on PVDF membranes. Five percent non-fat milk was used to block the membranes and then they were incubated with primary antibodies against SETD2, proliferating cell nuclear antigen (PCNA), Ki67, matrix metalloproteinase-2 (MMP-2), matrix metalloproteinase-9 (MMP-9), Caspase-3, Caspase-9 and β-actin at a 1:1000 dilution. We used secondary antibodies, horseradish peroxidase (HRP)-conjugated at a 1:5000 dilution. Molecular weight markers were present during electrophoresis. We used enhanced chemiluminescence to see the protein bands. ImageJ software (NIH, Bethesda, MD, USA) (Schneider et al., 2012) was used for densitometric analysis and the levels of target protein expression were adjusted to those of β-actin.

Statistical analysis

Statistical analysis was conducted using SPSS 19.0. Results were sub-grouped by average ± SD. All data were evaluated for normality before statistical analysis. Two-sided paired Student's t tests were used to compare matched tumor and adjacent normal tissues. An unpaired Student's t-test was used to compare two independent groups in cell-based studies. For comparisons among multiple groups, a one-way ANOVA and post hoc tests were performed. Relationships between variables were explored using Pearson's correlation analysis (Schober et al., 2018). The Kaplan–Meier survival curve shown in the manuscript were derived from previously published datasets and was not analyzed for the same study population. Correcting for multiple testing across independent experiments was not performed and thus, multi-group comparisons should be considered exploratory. $p<0.05$ was considered statistically significant.

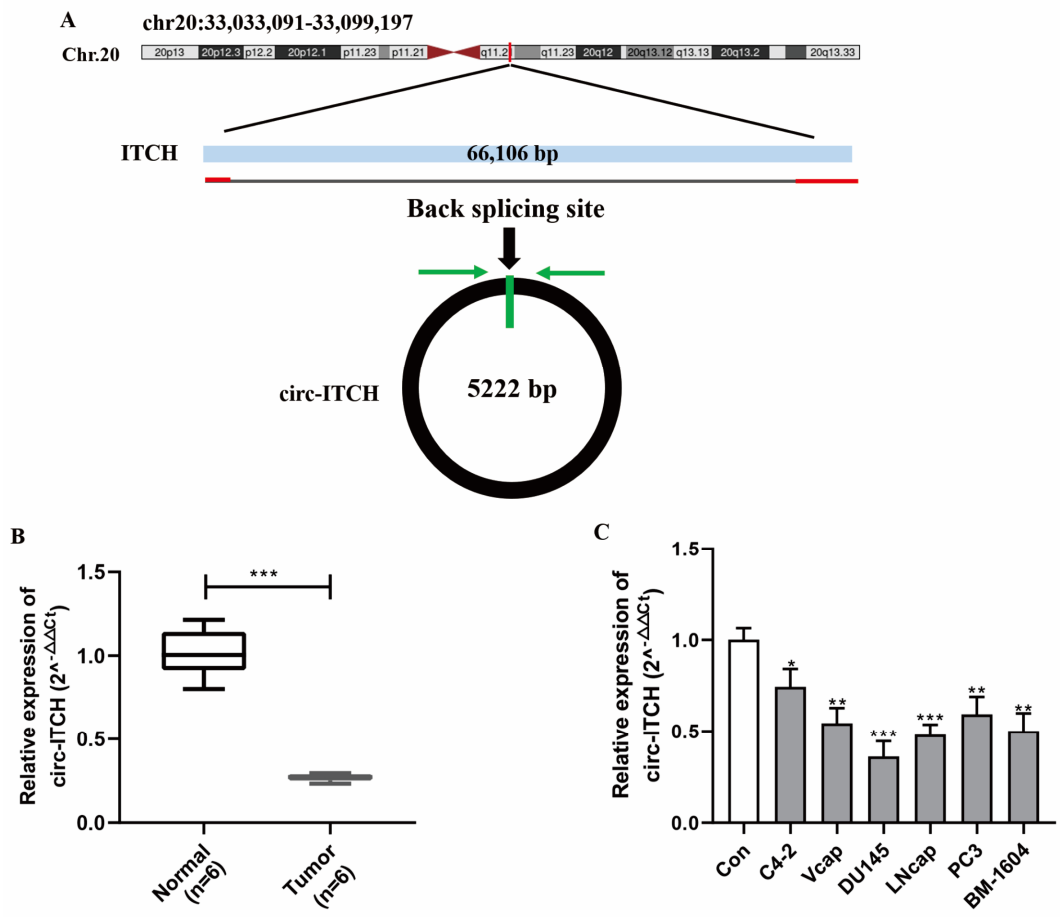

Fig. 1: circ-ITCH is down-regulated in PCa tissues and cell lines; (A) Schematic illustrating the genomic location of ITCH gene on chromosome 20 and generation of circ-ITCH through back-splicing by a green arrow; (B) The relative expression of circ-ITCH in prostate cancer tissues (Tumor) and adjacent normal tissues (Normal, n = 6 paired samples) was evaluated by qRT–PCR. Values are expressed as the mean ± SD. Statistical analysis were evaluated by paired Student's t-test (*P < 0.05, **P < 0.01, ***P< 0.001); (C) The relative expression of circ-ITCH in prostate cancer cell lines (C4-2, VCaP, DU145, LNCaP, PC3 and BM-1604) compared with RWPE-1 normal prostate epithelial cells detected by qRT–PCR. Values are means ± SD of three independent biological replicates (n = 3).

RESULTS

circ-ITCH in PCa tissues and cell repression of lines

Previous studies (Yang et al., 2018) have demonstrated that circ-ITCH is underexpressed across a range of malignancies and likely functions as a tumor suppressor. Based on these findings, we assessed the expression of circ-ITCH in PCa. Circ-ITCH is produced through exons back-splicing of ITCH gene and comprises 5,222 bp in sequence length at chr20:33033091–33099197 (Fig. 1A). Quantitative real-time PCR analysis of circ-ITCH in six pairs of prostate cancer and corresponding normal adjacent tissue specimens (n = 6). Clinicopathological features were described for illustration and the small number of cases was not analyzed statistically. Significant down-expression of circ-ITCH was observed in the PCa tissues, relative to matched adjacent normal tissues (Fig. 1B). Circ-ITCH was also downregulated in prostate cancer cell lines (C4-2, VCaP, DU145, LNCaP and PC3 and BM-1604) compared to the nonmalignant RWPE-1 normal prostate epithelial cells (Fig. 1C), suggesting a link between low circ-ITCH expression and prostate cancer at the cellular level.

Circ-ITCH inhibits PCa cell proliferation and apoptosis in-vitro induces

Based on the low expression of circ-ITCH in PCa tissues and cells, gain-of-function assays were conducted by overexpressing circ-ITCH in C4-2 and DU145 cells. The overexpression efficiency was validated by qRT-PCR analysis (their fold change is displayed in figs. 2A and 2B). CCK-8 analysis also revealed decreased metabolic activity in circ-ITCH– overexpressing cells relative to control cells (Figs. 2A and 2B). The CCK-8 assay measures metabolic activity, which serves as an indicator of cell viability rather than absolute cell numbers. Colony formation assays also demonstrated that circ-ITCH up-regulation markedly decreased clonogenic potential (Fig. 2C and D).

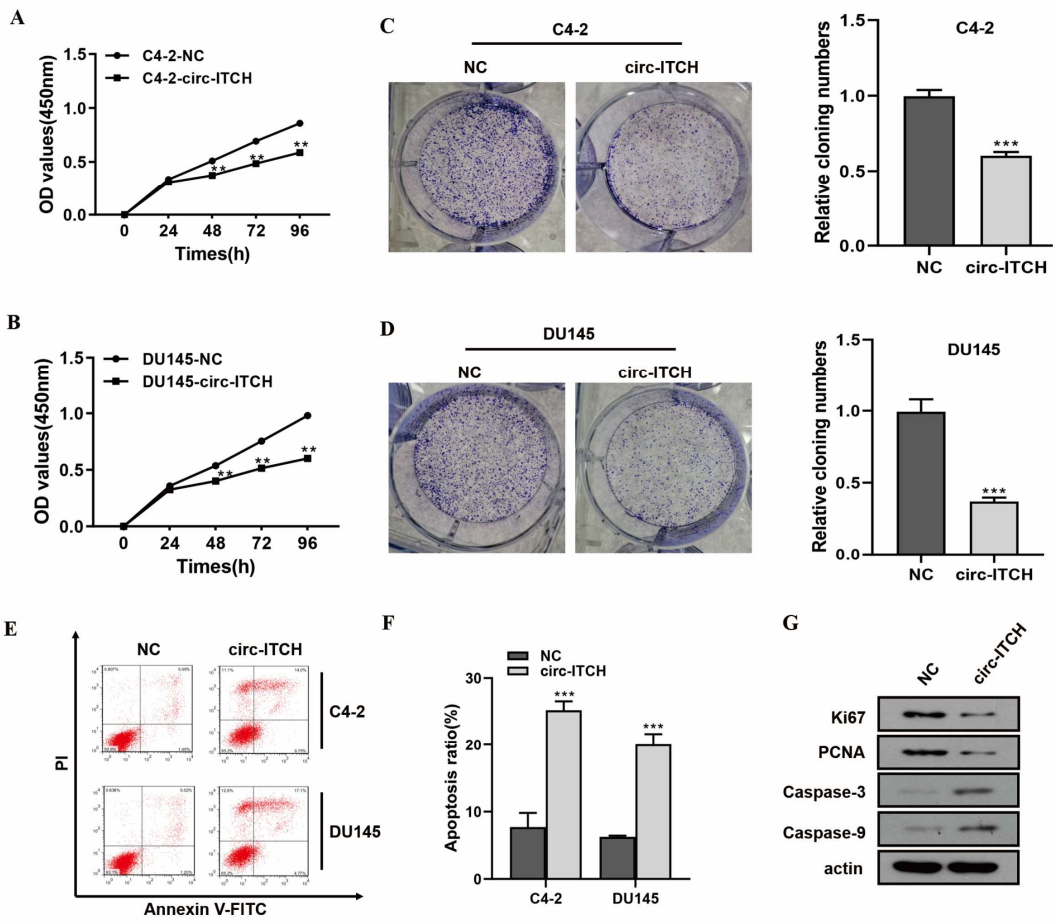

Fig. 2: circ-ITCH inhibits proliferation-associated phenotypes and enhances apoptosis in prostate cancer cells in vitro; (A and B) Cell viability-related metabolic activity of C4-2 and DU145 cells post-circ-ITCH overexpression, evaluated by CCK-8 assay at specified time points (mean ± SD, n = 3 independent biological replicates); (C and D) Representative images and quantification of colony formation assays indicate diminished clonogenic capacity in circ-ITCH–overexpressing cells (colonies with >50 cells were counted manually; mean ± SD, n = 3); (E and F) Flow cytometry analysis of apoptosis in C4-2 and DU145 cells subsequent to circ-ITCH overexpression, illustrating the ratios of early and late apoptotic cells (≥10,000 events analyzed per sample; mean ± SD, n = 3); (G) Western blot analysis of proteins related to proliferation (PCNA, Ki67) and apoptosis (cleaved caspase-3 and caspase-9). The loading control was β-actin. ImageJ software was used to do densitometric quantification, and the results were compared to β-actin (mean ± SD, n = 3). Unpaired Student's t-tests used to find out if the differences between the two groups were statistically significant (*P < 0.05, **P < 0.01, ***P < 0.001).

Flow cytometry revealed a markedly higher percentage of apoptotic cells, including both early- and late-apoptotic fractions, in circ-ITCH–overexpressing cells (Figs. 2E and F). β-Tubulin was used as a protein loading control (Fig. 2G). These findings collectively suggest that circ-ITCH regulates proliferation and apoptosis in PCa cells *in-vitro*.

Circ-ITCH inhibits PCa cell proliferation and induces apoptosis in-vitro

Furthermore, upregulation of circ-ITCH significantly attenuated the migratory and invasive abilities of C4-2 and DU145 cells, as measured by Transwell migration and invasion assays (Figs. 3A and 3B). These findings were further validated by wound healing assays (Figs. 3C–F). These serum-free media to avoid the impact of cellular proliferation. Furthermore, qRT-PCR and Western blot analysis showed that circ-ITCH upregulation was correlated with decreased mRNA and protein levels of MMP-2 and MMP-9, respectively (Figs. 3G and 3H). These molecular changes, which affect cell migration and invasion, suggest that circ-ITCH may modulate the phenotypes of PCa cells *in vitro*, rather than directly influencing tumorigenesis.

Relationship between circ-ITCH, miR-106b-5p and SETD2 regulation

Bioinformatic analyses suggested that miR-106b-5p binds to circ-ITCH. In PCa tissues, there was an inverse expression pattern between circ-ITCH and miR-106b-5p (Figs. 4A and 4B).

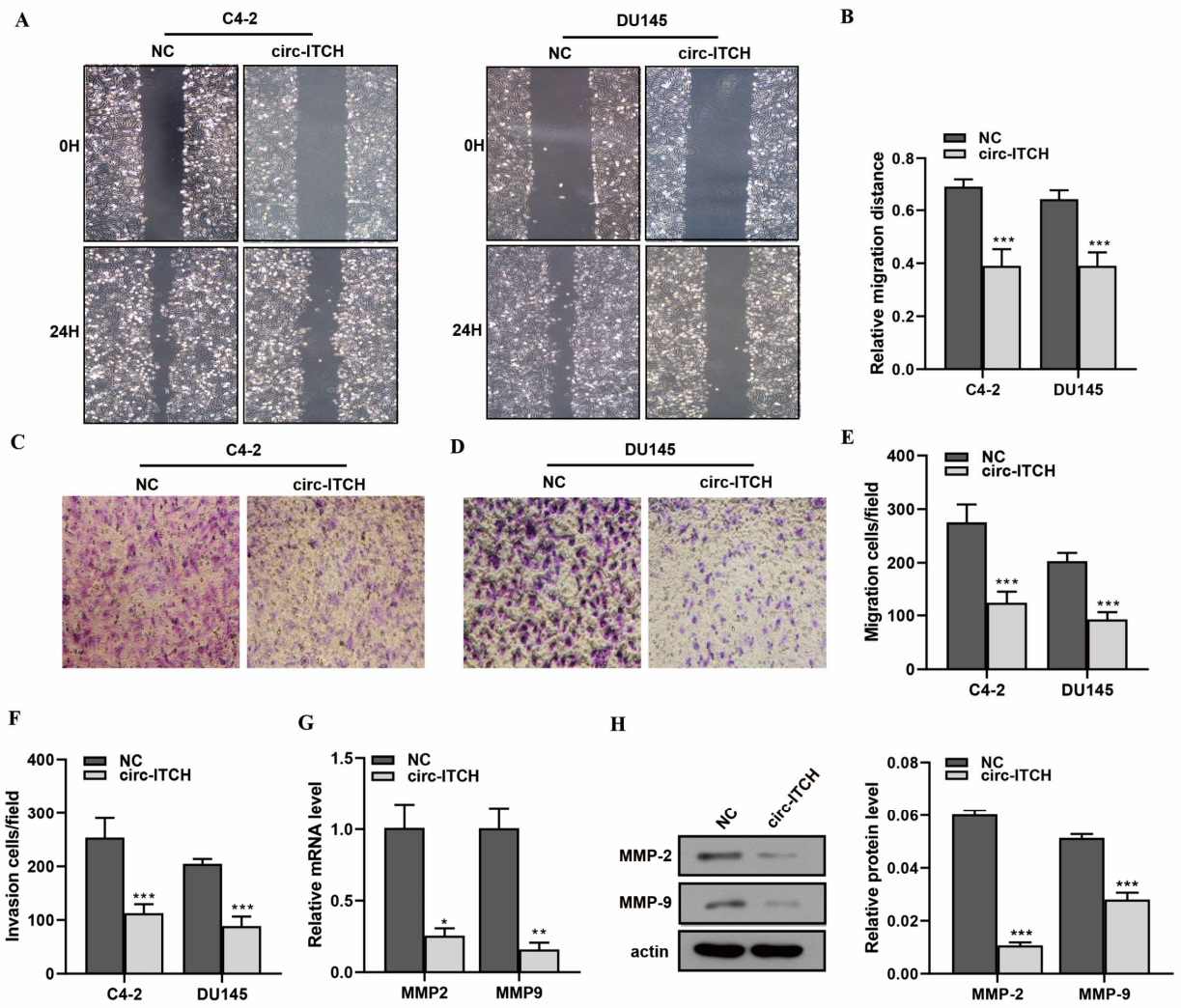

Fig. 3: circ-ITCH inhibits migration and invasion phenotypes of prostate cancer cells *in-vitro*. (A and B) Representative images and quantitative analysis of wound-healing assays in C4-2 and DU145 cells subsequent to circ-ITCH overexpression. We used ImageJ software to find the percentage of gap reduction relative to 0 h (mean ± SD, n = 3) to find the wound closure; (C-F) Representative images and quantification of Transwell migration and invasion assays (five random microscopic fields per insert were analyzed at ×200 magnification; mean ± SD, n = 3); (G) qRT–PCR was used to measure the relative levels of mRNA for MMP-2 and MMP-9 (mean ± SD, n = 3); (H) Protein expression levels of MMP-2 and MMP-9 evaluated through Western blot analysis, normalized densitometrically to β-actin (mean ± SD, n = 3). For comparing two groups, unpaired Student's t-tests were used for statistical analysis (*P < 0.05, **P < 0.01, ***P < 0.001).

The dual-luciferase reporter assays showed that miR-106b-5p mimics greatly lowered the luciferase activity of the circ-ITCH wild-type reporter, but there was no significant change in the mutant reporter (Fig. 4C). In C4-2 and DU145 cells, higher levels of circ-ITCH were linked to lower levels of miR-106b-5p (Fig. 4D). Bioinformatic predictions also pointed to SETD2 as a possible target of miR-106b-5p. This finding was supported by luciferase reporter assays, which showed that the wild-type SETD2 3'-UTR reporter exhibited reduced activity upon transfection with a miR-106b-5p mimic (Fig. 4E-F). Furthermore, SETD2 expression was down-regulated in prostate cancer tissues compared with adjacent normal tissues (Fig. 4G). Furthermore, circ-ITCH overexpression led to an elevation of SETD2 protein in DU145 cells (Figs. 4H and 4I), suggesting a relationship between circ-ITCH and SETD2. These results suggest that miR-106b-5p and SETD2 are reciprocally regulated in PCa cells.

The circ-ITCH/miR-106b-5p/SETD2 axis in-vitro changes the phenotypes related to proliferation, apoptosis, migration and invasion

Western blot analysis showed that circ-ITCH and SETD2 overexpression were associated with reduced expression of proliferation-related proteins (PCNA, Ki67) and migration-associated proteins (MMP-2, MMP-9).

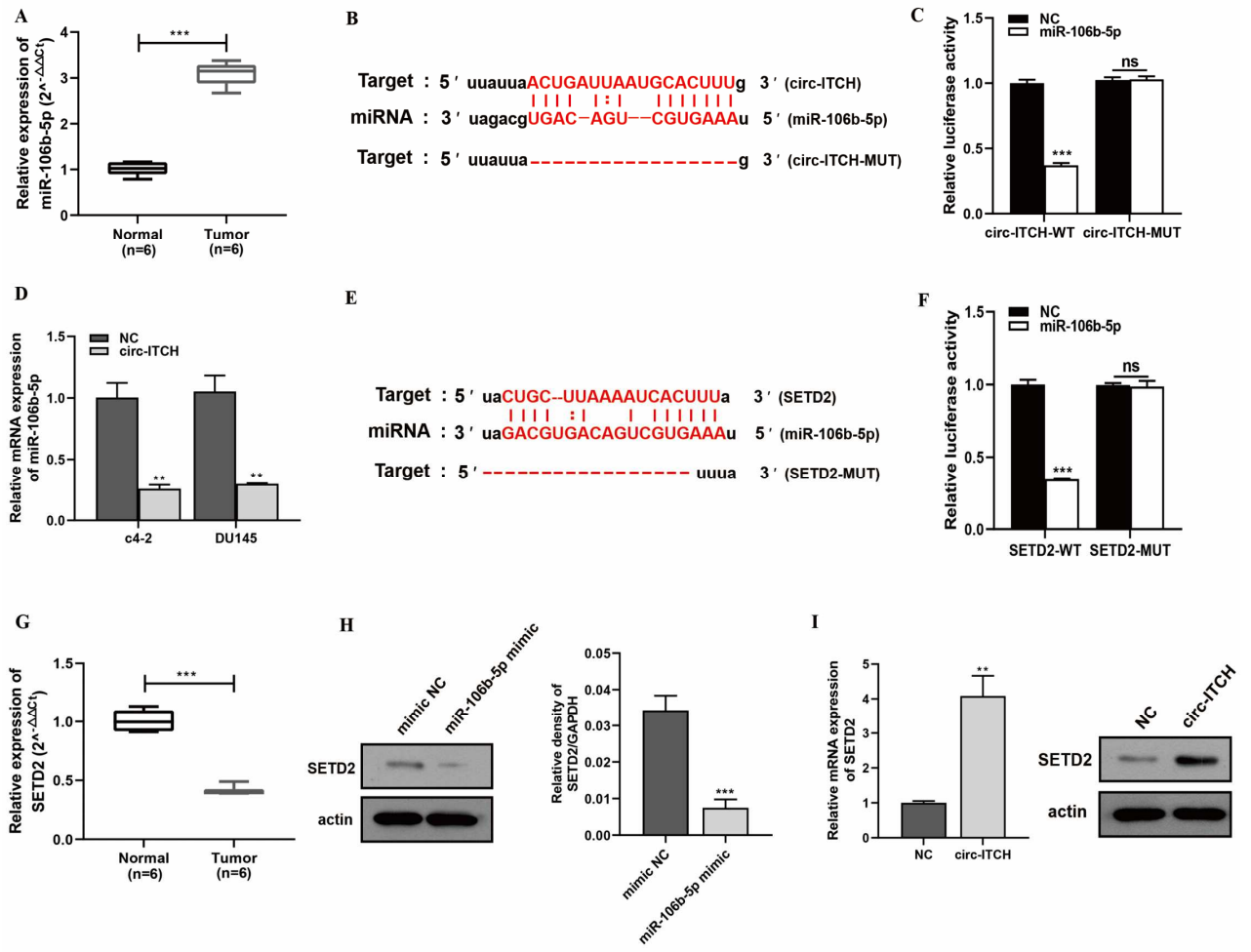

Fig. 4: circ-ITCH is linked to the regulation of SETD2 by miR-106b-5p; (A) Relative levels of miR-106b-5p expression in prostate cancer tissues and corresponding adjacent normal tissues assessed by qRT–PCR (n = 6 paired samples; mean ± SD; paired Student's t-test); (B) Anticipated interaction sites between circ-ITCH and miR-106b-5p; (C) A dual-luciferase reporter assay showing that the luciferase activity of circ-ITCH wild-type (WT) reporters went down after miR-106b-5p mimic transfection, but there was no significant change in mutant (MUT) reporters. The activity of firefly luciferase was adjusted to match the activity of Renilla luciferase (mean ± SD, n = 3); (D) Comparative expression levels of miR-106b-5p in C4-2 and DU145 cells subsequent to circ-ITCH overexpression (mean ± SD, n = 3); (E) Anticipated miR-106b-5p binding locus in the SETD2 3′-UTR; (F) A dual-luciferase reporter assay that confirms SETD2 as a possible target of miR-106b-5p (Firefly normalized to Renilla; mean ± SD, n = 3); (G) Relative SETD2 mRNA expression levels in prostate cancer tissues versus adjacent normal tissues (n = 6 paired samples; mean ± SD; paired Student's t-test); (H and I) Western blot analysis demonstrating elevated SETD2 protein expression subsequent to circ-ITCH overexpression in DU145 cells, with densitometric normalization to β-actin (mean ± SD, n = 3).

On the other hand, miR-106b-5p overexpression decreased the levels of pro-apoptotic proteins (cleaved caspase-3 and caspase-9) (Fig. 5A). Co-transfecting with miR-106b-5p mimics partially reversed the effects of circ-ITCH overexpression, suggesting a functional interaction between these molecules. CCK-8 assays showed that circ-ITCH overexpression attenuated the miR-106b-5p-induced increase in metabolic activity. Additionally, SETD2 overexpression promoted apoptosis, as evidenced by increased apoptotic cell populations (Figs. 5B, C). Transwell migration and invasion assays showed that modulation of circ-ITCH, miR-106b-5p and SETD2 significantly altered the migratory and invasive capacities of DU145 cells (Fig 5D). These results support the idea that the circ-ITCH/miR-106b-5p/SETD2 axis plays a regulatory role *in-vitro*.

DISCUSSION

The result of the current study indicated that circ-ITCH expression was decreased in prostate cancer tissues and cell lines, while overexpression of circ-ITCH adjusted proliferation-, apoptosis-, migration- and invasion-related cellular phenotypes of prostate cancer cells *in-vitro* (Hu and Guo, 2020; Cao *et al.,* 2022).

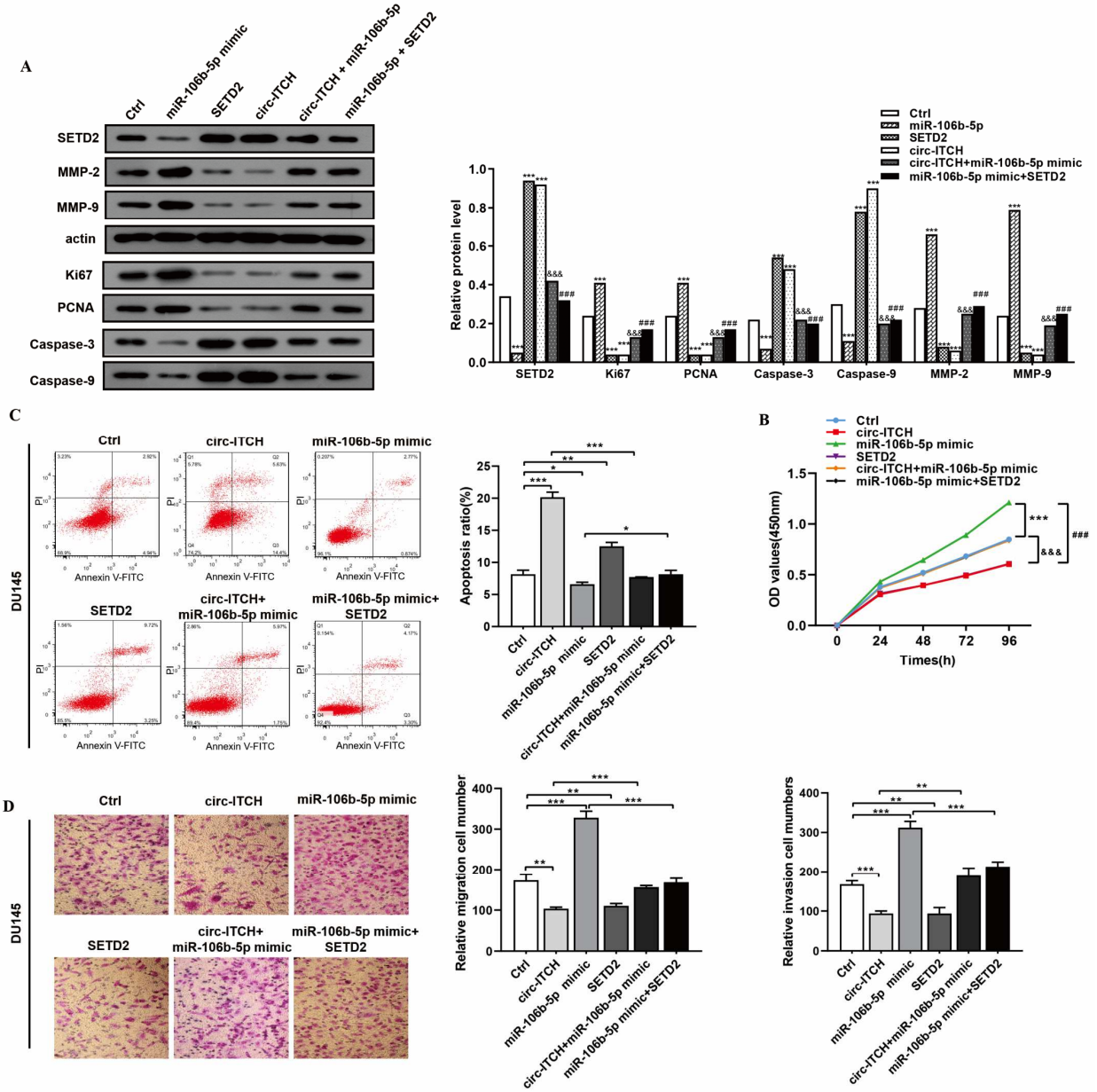

Fig. 5: circ-ITCH/miR-106b-5p/SETD2 axis regulates in vitro the malignant cellular behaviors of prostate cancer cells. (A) Levels of proliferation-associated proteins (PCNA, Ki67), apoptosis-related proteins (cleaved caspase-3 and caspase-9), or migration-related proteins (MMP-2 and MMP-9) were determined by western blot in DU145 cells with altered circ-ITCH expression, miR-106b 5p expression as well as SETD2 contents. The internal loading control was β-actin. Densitometric values were normalized to β-actin (mean ± SD, n = 3 independent biological replicates); (B) CCK-8 assay displayed differences of the metabolite activities when co-transfected with circ-ITCH, miR-106b-5p mimics or SETD2 plasmids (mean ± SD, n = 3); (C) Apoptotic cell population profiles in representative flow cytometry analyses of indicated treatment conditions (≥10,000 events analyzed per sample; mean ± SD, n = 3); (D) Transwell migration and invasion assays were used to analyze the migratory and invasive ability of DU145 cells after the regulation of circ-ITCH/miR-106b-5p/SETD2 (mean ± SD, n = 3). Statistical procedures to analyze multiple-group comparisons were conducted by the one-way ANOVA and followed by the post hoc test. Data are expressed as mean ± SEM, statistical annotations (*, ###, &&&) represent the defined comparisons among experimental groups; $P < 0.05$ was considered significant.

These results are concordant with those reported previously, indicating that circ-ITCH functions as a tumor suppressor in multiple cancer types (Ghafouri-Fard *et al.,* 2021; Li *et al.,* 2023; Liu *et al.,* 2022). As noted, these new findings, which differ from our established knowledge, are not the repetition of clinical relevance l circRNA–miRNA–mRNA regulatory relationships in prostate cancer cells (Wu *et al.,* 2020).

Several previous reports have shown that circ-ITCH downregulation is associated with poor clinicopathological features and unfavorable prognosis in PCa patients (Huang *et al.,* 2019). Nevertheless, these findings were derived from independent clinical cohorts and should not be directly compared with the current work, as it was restricted to in vitro functional assays and a small set of exploratory tissues. While previous studies proposed that circ-ITCH may be associated with pathological T stage and lymph node status(Huang, Chen and Yuan, 2019), this study lacks an investigation of the clinical progression or metastatic characteristics to which these cellular observations can directly apply.

Circ-ITCH has been reported as a competing endogenous RNA in other cancer types; for example, it was shown to be associated with the regulation of miR-17-5p and HOXB13 in prostate cancer (Wang *et al.,* 2019). The present study deliberately focused on its interaction with miR-106b-5p, without addressing all other reported functions, to avoid confounding effects from distinct signaling pathways. This focused approach allowed us to evaluate a previously underappreciated regulatory mechanism that is physiologically relevant to prostate cancer cells.

In this study, bioinformatics prediction combined with luciferase reporter assays revealed a circ-ITCH/miR-106b-5p axis and an inverse expression pattern was observed between these two regulatory molecules in prostate cancer tissues and cell lines. Here, miR-106b-5p is known to function as an oncogenic miRNA in various cancers, including colorectal and renal cancers, primarily by promoting cell proliferation and invasion (Ni *et al*., 2014; Slaby *et al.,* 2010). In the present study, increased expression of miR-106b-5p was associated with enhanced proliferative capacity and reduced apoptosis in PCa cells; both of these influences could be partially counteracted by circ-ITCH overexpression in vitro. These results, however, only suggest evidence (Hu and Guo, 2020).

SETD2 was identified as a downstream target of miR-106b-5p by bioinformatic prediction and verified by luciferase reporter assays. SETD2 is a histone-modifying enzyme that specifically trimethylates H3K36, thereby preserving genomic stability and ensuring transcription fidelity (Zhang *et al.,* 2015). SETD2 was downregulated in PCa tissues as previously reported and overexpression of acirc-ITCH led to the upregulation of SETD2 expression in PCa cells, indicating a downstream targeting relationship via miR-106b-5p (Yuan *et al.,* 2020).

These results are consistent with previous reports linking decreased SETD2 activity to aggressive cellular behavior through upstream regulatory mechanisms, although the underlying mechanisms remain poorly understood.

Rescue assays revealed that transfection with miR-106b-5p mimics counteracted the effects of circ-ITCH overexpression in prostate cancer cells, indicating a functional correlation within this putative regulatory circuit. Nevertheless, the reversal was incomplete and reciprocal SETD2 knockdown experiments yielded inconclusive results. Thus, further experiments are required to establish the hierarchical order of this pathway. It should be noted that the circ-ITCH/miR-106b-5p/SETD2 axis observed in this work is not only experimentally supported but also likely represents a promising regulatory network.

Some limitations need to be recognized in the report. Firstly, we restricted our sample size of human tissues (n = 6) in this study and as such had a lack of statistical strength that could not support extensive clinicopathological correlation analysis.

Second, only circ-ITCH overexpression was investigated in this study and there were no experiments to test the endogenous function of reciprocal loss-of function digestion and circ-ITCH. Third, validation of key circRNA, including RNase R resistance assay and Sanger sequencing of the back-spliced junction, was not performed. Fourth, no strict correction for multiple comparisons was applied in multi-group analyses. Finally, all functional assays were performed *in-vitro* and no *in-vivo* experiments were performed to assess tumor growth or metastatic behavior (Huang *et al.,* 2022). These limitations illustrate the necessity for further studies with larger patient cohorts, circ-ITCH knockdown methods, circRNA detectionwith techniques and animal experiments to confirm and expand these present findings.

CONCLUSION

circ-ITCH is down regulated in prostate cancer tissues and cell lines. *In-vitro* functional assays demonstrated that circ-ITCH overexpression suppresses the invasive capacity of prostate cancer cells. The results indicate a regulatory relationship between mediated circ-ITCH and SETD2, potentially modulated by circ-ITCH-mediated miR-106b-5p. Because the tissue analysis was exploratory and models used were exclusively *in-vitro*, these results are preliminary. More will help to define the biological role of *in-vivo* and mechanistic trials circ-ITCH/miR-106b-bp/SETD2 axis in prostate cancer.

Acknowledgments
This work was supported by grants from the National Natural Science Foundation of China (81902615). Science and Technology Projects in Guangzhou (202102080043, 202201010115, 202201020051). Science and Technology Planning for Basic Research Project of Guangzhou-Municipal School (Institution) Joint Funding (20220102060116).

Authors' contributions

Junbin Jiang: Designed the study; Longhong Ba, Jianwen We, Feicheng Chen, Yutong Li and Bin Pan: Performed experiments. All authors analyzed data and wrote the manuscript. All authors read and agree to publish the final version of the manuscript.

Funding

This study was supported by the Science and Technology Planning for Fundamental and Applied Basic Research of Guangzhou Municipal School (Institution) Joint Funding, Grant/Award Numbers: 2023A03J1012, 2024A03J1114 and 2025A03J4166.

Data availability statement

All of the data generated or analyzed during the present study are included in this article.

Ethical approval

This research protocol was reviewed and approved by the Medical Ethics Committee of the First Affiliated Hospital of Jinan University (Approval No. KY-2020-095). All procedures involving human specimens were performed in accordance with the Declaration of Helsinki.

Conflict of interest

The authors declare no conflict of interest.

REFERENCES

Cao C, Wang Y, Wu X, Li Z, Guo J and Sun W (2022). The roles and mechanisms of circular RNAs related to mTOR in cancers. *J. Clin. Lab. Anal.,* **36**(12): e24783.

de Bono J, Ramanathan RK, Mina L, Chugh R, Glaspy J, Rafii S, Kaye S, Sachdev J, Heymach J and Smith DC (2017). Phase I, dose-escalation, two-part trial of the PARP inhibitor talazoparib in patients with advanced germline BRCA1/2 mutations and selected sporadic cancers. *Cancer Discov.*, **7**(6): 620-629.

El-Aal AEA, Elshafei A, Ismail MY and El-Shafey MM (2023). Identification of MiR-106b-5p, MiR-601 and MiR-760 expression and their clinical values in non-small cell lung cancer (NSCLC) patients' serum. *Pathol. Res. Pract.*, **248**:154663.

Fontana F, Raimondi M, Marzagalli M, Di Domizio A and Limonta P (2020). Natural compounds in prostate cancer prevention and treatment: Mechanisms of action and molecular targets. *Cells*, **9**(2):460.

Ghafouri-Fard S, Khoshbakht T, Taheri M and Jamali E (2021). CircITCH: A circular RNA with eminent roles in the carcinogenesis. *Front. Oncol.,* **11**: 774979.

Granata A, Maccarrone R, Anzaldi M, Leonardi G, Pesce F, Amico F, Gesualdo L and Corrao S (2022). GLP-1 receptor agonists and renal outcomes in patients with diabetes mellitus type 2 and diabetic kidney disease: State of the art. *Clin. Kidney J.*, **15**(9):1657-65.

Gullaksen S, Vernstrøm L, Sørensen SS, Ringgaard S, Laustsen C, Funck KL, Poulsen PL and Laugesen E (2023). Separate and combined effects of semaglutide and empagliflozin on kidney oxygenation and perfusion in people with type 2 diabetes: A randomized trial. *Diabetologia*, **66**(5):813-825.

Gullaksen S, Vernstrøm L, Sørensen SS, Ringgaard S, Laustsen C, Birn H, Funck KL, Poulsen PL and Laugesen E (2024). The effects of semaglutide, empagliflozin and their combination on the kidney sodium signal from magnetic resonance imaging: A prespecified, secondary analysis from a randomized, clinical trial. *J. Diabetes Complicat.*, **38**(2):108673.

Hu J, Li X, Xu K, Chen J, Zong S, Zhang H, Li H, Zhang G, Guo Z, Zhao X, Jiang Y and Jing Z (2024). CircVPS8 promotes the malignant phenotype and inhibits ferroptosis of glioma stem cells by acting as a scaffold for MKRN1, SOX15 and HNF4A. *Oncogene,* **43**(36): 2679–2695.

Hu Y and Guo B (2020). Circ-MTO1 correlates with favorable prognosis and inhibits cell proliferation, invasion as well as miR-17-5p expression in prostate cancer. *J. Clin. Lab. Anal.,* **34**(3): e23086.

Huang E, Chen X and Yuan Y (2019). Downregulated circular RNA itchy E3 ubiquitin protein ligase correlates with advanced pathologic T stage, high lymph node metastasis risk and poor survival in prostate cancer patients. *Cancer Biomark.*, **26**(1):41-50.

Huang HB, Luo HT, Wei NN, Liu ML, He F, Yang W, Dong J, Yang XF and Li FR (2022). Integrative analysis reveals a lineage-specific circular RNA landscape for adipo-osteogenesis of human mesenchymal stem cells. *Stem Cell Res. Ther.,* **13**(1): 106.

Humphrey PA, Moch H, Cubilla AL, Ulbright TM and Reuter VE (2016). The 2016 WHO classification of tumours of the urinary system and male genital organs—part B: Prostate and bladder tumours. *Eur. Urol.*, **70**(1):106-119.

Huang E, Chen X and Yuan Y (2019). Downregulated circular RNA itchy E3 ubiquitin protein ligase correlates with advanced pathologic T stage, high lymph node metastasis risk and poor survival in prostate cancer patients. *Cancer Biomark.,* **26**(1): 41-50.

Kapper C, Oppelt P, Arbeithuber B, Gyunesh AA, Vilusic I, Stelzl P and Rezk-Füreder M (2024). Targeting ferroptosis in ovarian cancer: Novel strategies to overcome chemotherapy resistance. *Life Sci.,* **349**: 122720.

Li X, Yin X, Bao H and Liu C (2023). Circular RNA ITCH increases sorafenib-sensitivity in hepatocellular carcinoma via sequestering miR-20b-5p and modulating the downstream PTEN-PI3K/Akt pathway. *Mol. Cell. Probes.,* **67**: 101877.

Liu T, Huang T, Shang M and Han G (2022). CircRNA ITCH: Insight into its role and clinical application prospect in tumor and non-tumor diseases. *Front. Genet*., **13**: 927541.

Lucarini V, Nardozi D, Angiolini V, Benvenuto M, Focaccetti C, Carrano R, Besharat ZM, Bei R and Masuelli L (2023). Tumor microenvironment remodeling in gastrointestinal cancer: Role of MiRNAs as biomarkers of tumor invasion. *Biomedicines,* **11**(6)*:* 1761.

Mazzieri A, Porcellati F, Timio F and Reboldi G (2024). Molecular targets of novel therapeutics for diabetic kidney disease: A new era of nephroprotection. *Int. J. Mol. Sci.*, **25**(7): 3969.

Nabar N, Dacoba TG, Covarrubias G, Romero-Cruz D and Hammond PT (2024). Electrostatic adsorption of polyanions onto lipid nanoparticles controls uptake, trafficking and transfection of RNA and DNA therapies. *Proc. Natl. Acad. Sci.,* **121**(11): e2307809121.

Neri F, Rapelli S, Krepelova A, Incarnato D, Parlato C, Basile G, Maldotti M, Anselmi F and Oliviero S (2017). Intragenic DNA methylation prevents spurious transcription initiation. *Nature*, **543**(7643):72-77.

Pan X, Chen K, Gao W, Xu M, Meng F, Wu M, Wang ZQ, Li YQ, Xu W, Zhang M and Luo Y (2025). Circular RNA circBNC2 inhibits tumorigenesis by modulating ferroptosis and acts as a nanotherapeutic target in prostate cancer. *Mol. Cancer,* **24**(1): 29.

Plym A, Zhang Y, Stopsack KH, Ugalde-Morales E, Seibert TM, Conti DV, Haiman CA, Baras A, Stocks T, Drake I and Penney KL (2024). Early prostate cancer deaths among men with higher vs lower genetic risk. *JAMA Netw. Open,* **7**(7): e2420034.

Rawla P (2019). Epidemiology of prostate cancer. *World J. Oncol.*, **10**(2):63-89.

Schneider CA, Rasband WS and Eliceiri KW (2012). NIH Image to ImageJ: 25 years of image analysis. *Nat. Methods*, **9**: 671-675.

Schober P, Boer C and Schwarte LA (2018). Correlation coefficients: Appropriate use and interpretation. *Anesth Analg*., **126**(5): 1763-1768.

Slaby O, Jancovicova J, Lakomy R, Svoboda M, Poprach A, Fabian P, Kren L, Michalek J and Vyzula R (2010). Expression of miRNA-106b in conventional renal cell carcinoma is a potential marker for prediction of early metastasis after nephrectomy. *J. Exp. Clin. Cancer Res.*, **29**(1): 90.

Shi Y, Guo Z, Fang N, Jiang W, Fan Y, He Y, Ma Z and Chen Y (2019). hsa_circ_0006168 sponges miR-100 and regulates mTOR to promote the proliferation, migration and invasion of esophageal squamous cell carcinoma. Biomed. *Pharmacother.,* **117**: 109151.

Siegel RL, Giaquinto AN and Jemal A (2024). Cancer statistics, Cancer JC. 2024 Jan-Feb; **74**(1): 12–49.

Su K, Yi Q, Dai X and Liu O (2022). Circular RNA ITCH: an emerging multifunctional regulator. *Biomolecules,* **12**(3): 359.

Vidallon MLP, Liu H, Lu Z, Acter S, Song Y, Baldwin C, Teo BM, Bishop AI, Tabor RF, Peter K, de Campo L and Wang X (2024). Polydopamine nanobowl-armoured perfluorocarbon emulsions: Tracking thermal- and photothermal-induced phase change through neutron scattering. *Small,* 2025; **21**(2): e2406019.

Wang X, Wang R, Wu Z and Bai P (2019). Circular RNA ITCH suppressed prostate cancer progression by increasing HOXB13 expression via sponging miR-17-5p. *Cancer Cell Int.*, **19**:1-11.

Wu YP, Lin XD, Chen SH, Ke ZB, Lin F, Chen DN, Xue XY, Wei Y, Zheng QS, Wen YA and Xu N (2020). Identification of prostate cancer-related circular RNA through bioinformatics analysis. *Front. Genet.,* **11**: 892.

Yang C, Yuan W, Yang X, Li J, Wang Y and Zhang L (2018). Circular RNA circ-ITCH inhibits bladder cancer progression by sponging miR-17/miR-224 and regulating p21, PTEN expression. *Mol. Cancer,* **17**(1): 19.

Yerukala Sathipati S, Tsai MJ, Shukla SK and Ho SY (2023). Artificial intelligence-driven pan-cancer analysis reveals MiRNA signatures for cancer stage prediction. *Hum. Genet. Genom. Adv.*, **4**: 100190.

Yuan H, Han Y, Wang X, Li N, Liu Q, Yin Y, Wang H, Pan L, Li L and Song K (2020). SETD2 restricts prostate cancer metastasis by integrating EZH2 and AMPK signaling pathways. *Cancer Cell*, **38**(3): 350-365.e7.

Zhang GJ, Li JS, Zhou H, Xiao HX, Li Y and Zhou T (2015). MicroRNA-106b promotes colorectal cancer cell migration and invasion by directly targeting DLC1. *J. Exp. Clin. Cancer Res.*, **34**(1): 73.

Zhang J, Liu L, Wei X, Zhao C, Li S, Li J and Le TD (2023). Pan-cancer characterization of NcRNA synergistic competition uncovers potential carcinogenic biomarkers. *PLoS Comput. Biol.*, **19**(10): e1011308.

Zhang Z, Gao Z, Fang H, Zhao Y and Xing R (2024). Therapeutic importance and diagnostic function of circRNAs in urological cancers: From metastasis to drug resistance. *Cancer Metastasis Rev.,* **43**(3): 867–888.

Zhong D, Wang Z, Ye Z, Wang Y and Cai X (2024). Cancer-derived exosomes as novel biomarkers in metastatic gastrointestinal cancer. *Mol. Cancer,* **23**(1): 67.

Zhou Q, Meng Y, Li D, Yao L, Le J, Liu Y, Sun Y, Zeng F, Chen X and Deng G (2024). Ferroptosis in cancer: From molecular mechanisms to therapeutic strategies. *Signal Transduct. Target Ther.,* **9**(1): 55.